Journal of Non-Newtonian Fluid Mechanics 167–168 (2012) 9–17

Contents lists available at SciVerse ScienceDirect

Journal of Non-Newtonian Fluid Mechanics

journal homepage: http://www.elsevier.com/locate/jnnfm

Squeeze flow behavior of (soft glassy) thixotropic material

Asima Shaukat, Ashutosh Sharma, Yogesh M. Joshi *

Department of Chemical Engineering, Indian Institute of Technology Kanpur, Kanpur 208 016, India

ARTICLE INFO

Article history:
Received 16 June 2011
Received in revised form 16 September 2011
Accepted 23 September 2011
Available online 1 October 2011

Keywords:
Squeeze flow
Laponite suspension
Herschel–Bulkley fluid
Thixotropy
Physical aging
Rejuvenation

ABSTRACT

We study the flow behavior of a model soft glassy material – an aqueous suspension of Laponite – when it is squeezed between two circular parallel plates of different roughness. Aqueous suspension of Laponite shows a time dependent aging behavior as reflected in increased elastic modulus as well as yield stress, both of which however also decrease with an increase in the strength of deformation field thereby demonstrating typical thixotropic character. In a squeeze flow situation, under both force as well as velocity controlled modes; we find the behavior to be independent of the initial gap between the plates. In a constant force mode, the gap between the plates decreases until it reaches a finite limiting value, which is found to increase with an increase in age of the material as well as with a decrease in the applied force. In constant velocity experiments, at large gaps between the plates, normal force varies inversely with plate separation. The normal force is higher for a sample aged for a longer time as well as for a larger velocity of the top plate. We observe that the experimental behavior follows prediction of Herschel–Bulkley model solved for the squeeze flow (with different friction coefficients at the two plates) reasonably well under weak deformation fields. However, under strong deformation fields, experimental behavior deviates significantly from the prediction of Herschel–Bulkley model. This deviation arises due to melting or partial yielding of Laponite suspension under large deformation fields causing decrease in the viscosity, elastic modulus and the yield stress.

1. Introduction

Many biologically and commercially important soft materials undergo evolution of their structure and rheological properties as a function of time. Typically such materials demonstrate increase in viscosity and elastic modulus under quiescent conditions [1–3]. Under application of deformation field having sufficient strength, viscosity and elastic modulus decrease as a function of time [4–7]. In rheology literature this behavior is represented by a term: thixotropy [8,9]. Physically, the time dependent behavior is usually attributed to kinetic infeasibility of these materials to attain thermodynamic equilibrium over the experimental time-scales. Consequently, the exploration of the available phase space in search of lower energy states drives the thixotropic materials to undergo evolution of their structure as a function of time. In the recent literature, this phenomenon is termed as physical aging [6,10–14], while decrease in viscosity and elastic modulus as a function of time under application of deformation field is termed as rejuvenation. Owing to the behavioral similarity, which this class of materials share with the structural glasses, these are represented as soft glassy materials [15]. The thixotropic behavior (or aging and rejuvenation) imparts strong history dependence and influence any commercial processing of these materials necessary to form a useful product. Therefore, better understanding of the rheological behavior of these materials, particularly through more realistic flow fields, is desirable.

Squeeze flow is an important flow field often encountered in materials processing [16] and biology [17]. Material is compressed between two parallel plates in a squeeze flow, either by applying a compressive force [18] or by maintaining a constant velocity [19,20] so that a radial flow is produced. Squeeze flows of inelastic and visco-elastic fluids have been extensively studied by theory, simulations and experiments [16]. This class of rheometry is cost effective and can be particularly useful for materials which are too stiff or viscous to be handled with conventional rheometer geometries. Due to its commercial importance and academic interest, the study of yield stress fluids under squeeze flow conditions has generated considerable interest. Though this rheological technique is operationally simple and convenient, the complexities of wall slip [21–23], unsheared regions between the plates [24–26], phase separation due to relative radial motion of various phases [27], can make interpretations more difficult than the conventional methods. Much of work on squeeze flow of yield stress fluids is associated with theoretically and experimentally analyzing the flow field vis-à-vis yielding surface which determines the size and shape of unyielded regions within the material which move as a plug [24,26,28], effect of the boundary characteristics like presence or absence of a slip between the plate–sample surface

* Corresponding author. Tel.: +91 512 2597993; fax: +91 512 2590104.
E-mail address: joshi@iitk.ac.in (Y.M. Joshi).

0377-0257/$ - see front matter © 2011 Elsevier B.V. All rights reserved.
doi:10.1016/j.jnnfm.2011.09.006

[29–31] and as a means of an estimation of various rheological properties of the material particularly the yield stress [28,32,33]. Most of the real fluids that possess the yield stress are thixotropic and show complicated rheological behavior for any simple mathematical model to work well. Nonetheless, in numerous studies it has been shown that many soft materials with yield stress can be satisfactorily modeled with Bingham or Herschel–Bulkley constitutive relation in which the material is modeled to possess an infinite viscosity until a threshold stress is reached beyond which it behaves like a 'power law' viscous fluid [18,20,32,34–37]. However, still in many cases these models prove to be rather simple in nature due to some important inadequacies. The most important one is that they are time independent in nature whereas yield stress fluids are more often than not thixotropic as well. The reason is that the same underlying phenomenon of presence/destruction of a microscopic structure gives rise to both [9]. Another difficulty is determining the exact value of the yield stress of the material, which has been a subject of much debate in the rheology community [38,39]. The reason for this is a strong dependence of the yield stress on the experimental procedure followed in order to determine it. Many models for thixotropic fluids have been proposed which take into account the evolution of a structural parameter with time which corresponds to the degree of flocculation, jamming or the fraction of particles trapped in energy wells [8,40–42].

In this work, we study squeeze flow with plates having different roughness. In industry plates having dissimilar roughness are used so that the material preferentially sticks to only one surface. Plates having dissimilar characteristics have also been used to study shear flow behavior of soft glassy materials [43]. We use an aqueous suspension of Laponite in the squeeze flow study. Laponite is an important additive used in the chemical and the food industry to control rheological behavior of the end product [44]. Aqueous suspension of Laponite not only shows yield stress [45], but also demonstrates various generic thixotropic characteristic features of soft glassy materials like: deformation field dependent and time dependent viscosity and elasticity (and therefore, relaxation time) [6,46], incomplete stress relaxation upon application of step strain [47], weak frequency dependence of modulus [48], etc. It is thus considered to be a model soft glassy material [7,14,45,49–56]. Apart from academic significance, understanding squeeze flow behavior of soft glassy (thixotropic) materials is important from an industrial point of view as well. Many commercial soft glassy materials such as highly filled polymer melt and wheat dough do undergo squeeze flow while forming useful products.

2. Material, sample preparation and viscometry

Laponite® is a synthetic hectorite clay and is composed of disk like particles with a diameter of 25 nm and thickness of 1 nm [44,57]. In this work, we have used a suspension of 3.5 wt.% Laponite RD (Southern Clay Products, Inc.) in water. The white powder of Laponite was dried for 4 h at 120 °C before mixing with water. The sample was prepared by mixing a calculated amount of Laponite RD with ultrapure water at pH 10 under continuous stirring. The suspension was stirred vigorously for 30 min and left undisturbed for 1 month in a sealed polypropylene bottle. In this work, we have carried out oscillatory shear experiments and both force controlled and velocity controlled squeeze flow experiments using Anton Paar Physica MCR 501 rheometer (parallel plate geometry, 50 mm diameter). Before starting each experiment, Laponite suspension was shear melted by first passing it through an injection syringe having 0.5 mm diameter needle and 4 cm length several times. Subsequently, after loading it in the parallel plate geometry of the rheometer, suspension was further shear melted by applying an oscillatory rotational shear stress which is higher than the yield stress. The aging time was measured after the shear melting was stopped. We have carried out most of the oscillatory as well as squeeze flow experiments using a rough sandblasted top plate (roughness: 5.74 μm), unless otherwise mentioned where a smooth polished top plate (roughness: 0.8 μm) was used. The bottom plate was a smooth polished plate (roughness: 0.8 μm) in all the experiments. The free surface of the sample between the plates was coated with low viscosity silicone oil to prevent evaporation and/or contamination with CO_2 [58]. All the experiments were carried out at 25 °C.

3. Results

Aqueous suspension of Laponite is known to undergo enhancement in elastic modulus and characteristic relaxation time as a function of time [7,48,59]. The suspension has paste like (soft solid) consistency and it also demonstrates yield stress [60]. We measure the yield stress of the suspension at various times elapsed after shear melting (aging time) by carrying out stress sweep oscillatory experiments at frequency $f = 1$ Hz. Fig. 1 shows that with increase in shear stress (σ_0), elastic modulus (G') decreases sharply over a very narrow range of stress amplitudes thereby enabling measurement of yield stress. We do not rule out the presence of thixotropy introducing an error in the determination of the yield stress but we expect it to be small as the rate of change of shear stress was high allowing completion of the whole experiment in a time span of the order of seconds. As the time required to carry out each stress sweep experiment was much smaller than the corresponding elapsed time (aging time), structural evolution (aging) that takes place during the course of experiment can be ignored. Interestingly, all the data obtained at different aging times show a superposition when elastic modulus is normalized by the elastic modulus associated with the linear response regime (G_0) and stress amplitude is normalized by the yield stress (τ_y). In the inset of Fig. 1, G_0 and τ_y are plotted as a functions of aging time (t_w). It can be seen that material demonstrates enhancement of modulus (G_0), and yield stress (τ_y) with the same dependence on aging time, $\tau_y,\ G_0 \propto t_w^{0.4}$ ($\tau_y \sim G_0$).

It has been shown that many soft glassy materials with yield stress can be satisfactorily modeled with Herschel–Bulkley constitutive relation given by [18,20,32,35]:

$$\underset{\approx}{\sigma} = \tau_y + k\dot{\gamma}^{n-1}\,\underset{\approx}{\dot{\gamma}}, \quad \text{if } (\underset{\approx}{\sigma} : \underset{\approx}{\sigma}/2 \geqslant \tau_y^2) \quad \text{and}$$

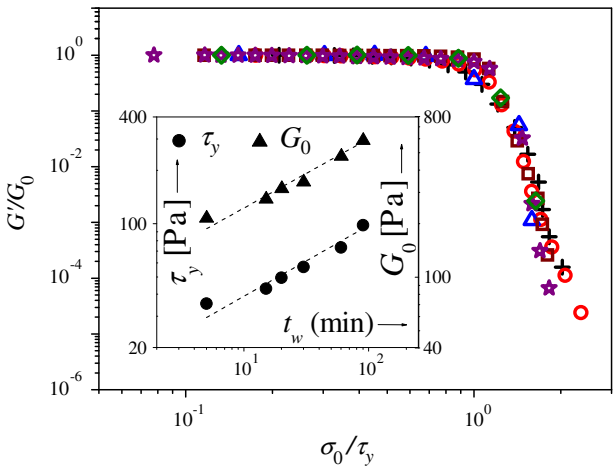

Fig. 1. Yielding behavior of Laponite suspension in a stress sweep oscillatory test at frequency $f = 1$ Hz for various aging times [square: 5 min, circle: 15 min, triangle: 20 min, diamond: 30 min, star: 60 min and plus: 90 min]. Inset shows yield stress (τ_y) and linear regime elastic modulus (G_0) plotted as a function of aging time (t_w). Both τ_y and G_0 follow the same dependence on t_w given by $\tau_y, G_0 \propto t_w^{0.4}$.

$$\dot{\underset{\approx}{\gamma}} = 0, \quad \text{if } (\underset{\approx}{\sigma} : \underset{\approx}{\sigma}/2 < \tau_y^2). \tag{1}$$

Here σ is the stress tensor, $\dot{\gamma}$ is the rate of strain tensor, while $\dot{\gamma}$ is a second invariant of the rate of strain tensor, k is a model parameter (consistency) and n is a flow index. In order to test rheological behavior of aqueous Laponite suspension from Herschel–Bulkley constitutive relation point of view, we carry out a simple shear rate ramp test and measure the shear stress as shown in Fig. 2. We indeed find that the behavior can be satisfactorily represented by a Herschel–Bulkley model with the values of n and k equal to 0.28 and 8 Pa s^n respectively for a sample aged for 15 min. However, since the material is thixotropic, its behavior is highly dependent on the flow field and the history (for example, for 15 min old Laponite suspension yield stress obtained from oscillatory experiment shown in Fig. 1 can be seen to be greater than that observed in shear rate ramp test shown in Fig. 2). Consequently, Herschel–Bulkley model parameters are also expected to be a function of the rate of change of shear rate and therefore one might obtain a different set of values of these parameters for a different rate of variation of the shear rate. In addition, since values of n and k are determined by using yield stress, these values are expected to be less accurate than the yield stress itself.

It should be noted that for all the squeeze flow experiments carried out in this study, the sample area remains constant throughout the experiment. The excess sample gets squeezed out from between the plates due to the decreasing gap, which leads to an accumulation of the sample outside the periphery of the plates. This may lead to a small but unknown pressure build up [16,61]. Nonetheless this arrangement is preferred because it gives an advantage of a known sample area at all the times.

In the first part of this work, we discuss the results of constant force mode experiments. In this mode, a constant compressive force is applied to the top plate and the evolution of gap (d) between the plates is recorded as a function of time (t). Fig. 3 shows d vs. t for two different arrangements: a rough top plate and a smooth bottom plate (black symbols) and both smooth plates (gray symbols). We find that in both the types of top plates, gap decreases rapidly in the beginning but eventually reaches a plateau. Only fluids with a yield stress are known to show a finite long-time separation, which has been used to determine yield stress of the material [28,32]. In addition the plateau associated with smooth top plate is observed to be lower than that of the rough top plate suggesting strong influence of boundary condition on the result. We first analyze this result from a point of view of Herschel–Bulkley model. An important dimensionless group for the flow of yield stress fluids is a plasticity number ($S = Vk^{1/n}R/(\tau_y^{1/n}d^2)$), where R is radius of the plate and V is velocity of the top plate. In the limit of small plasticity number, $S \ll 1$, which denotes a greater contribution of yield stress compared to viscous stress, and under the no-slip boundary condition, limiting gap (plateau) associated with Herschel–Bulkley fluid is given by [28]:

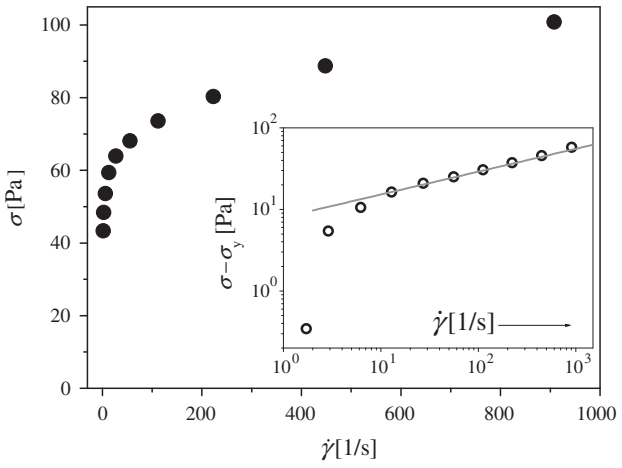

Fig. 2. Shear stress σ plotted as a function of shear rate $\dot{\gamma}$. In the inset we plot the difference between the shear stress and the yield stress ($\sigma - \sigma_y$) as a function of $\dot{\gamma}$ to determine the value of Herschel–Bulkley model parameters: flow index n and consistency k. The solid gray line which is the best fit for the data yields the value of k = 8 Pa s^n and n = 0.28. The top plate is rough while the bottom plate is smooth and t_w = 15 min. The time duration of the whole experiment is 84 s.

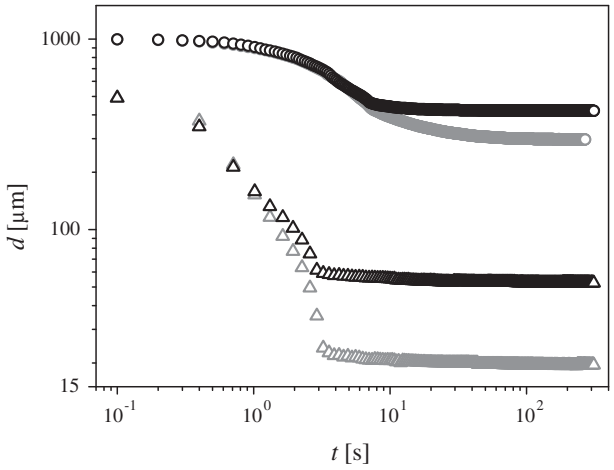

Fig. 3. Variation of gap (d) between the plates with time (t) for rough (black symbols) and smooth top plate (gray symbols) for two different compressive forces: F = 2.5 N (circles) and F = 10 N (triangles). The bottom plate was smooth for all the experiments and the aging time for all the cases shown is t_w = 15 min. The limiting gap d_L subsequent to which deformation ceases is always higher for the rough plate.

$$d_L = \frac{2\pi R^3 \tau_y}{3F}. \tag{2}$$

This limiting value of gap (d_L) has been used in the literature to predict the yield stress. The value of yield stress, calculated from Eq. (2) by substituting the value of d_L for the rough plate and F = 2.5 N, is a factor of 0.74 smaller than the yield stress predicted from the oscillatory shear stress ramp experiment shown in Fig. 1 for t_w = 15 min. It can be seen from Fig. 3 that d_L is much lower for a smooth plate than for a rough plate and consequently yield stress determined by the above method for a smooth plate for F = 2.5 N is even smaller. This discrepancy between the values of yield stress determined from the two squeeze experiments could be because of the presence of slip between the sample and the plate surfaces whose intensity increases when the top plate is changed from rough to smooth.

For a Herschel–Bulkley fluid, with a partial slip between the plate and the sample, Sherwood and Durban [62] defined a frictional stress at the interface to be a constant fraction of an effective Mises stress, which they referred to as the friction coefficient $m(\leqslant 1)$. They developed an expression for normal force when the friction coefficient m is same for both the plates [62]. For $d \ll R$, $m^2 \ll 1$ and $m \gg d/R$, the limiting gap for the Herschel–Bulkley fluid for partial slip is given by [33]:

$$d_L = \frac{2\pi R^3 m \tau_y}{3F}. \tag{3}$$

Therefore, when both the top and bottom plates are smooth, assuming material to behave as a Herschel–Bulkley fluid, friction coefficient can be estimated to be m = 0.53 for a compressive force of F = 2.5 N.

In order to develop an expression when the top and bottom plates have dissimilar roughnesses (or friction coefficients), we

carried out an exercise on the same lines as that of Sherwood and Durban [62,63] by considering different boundary conditions on both the surfaces given by a friction coefficient m_1 at the top plate and m_2 at the bottom plate. The details of the analysis are given in the Appendix. In the limit of $d \ll R$, $m_1^2, m_2^2 \ll 1$ and $m_1, m_2 \gg d/R$, the limiting gap is given by (by putting $V = 0$ in Eq. (A.32)):

$$d_L = \frac{\pi R^3 (m_1 + m_2)\tau_y}{3F}. \quad (4)$$

Substituting a value of $m_2 = 0.53$ in Eq. (4), which we have determined from the case in which both top and bottom plates are smooth, and from the value of d_L for rough top plate as shown in Fig. 3, we get $m_1 = 0.94$ (rough plate) for $F = 2.5$ N. Interestingly, for $F = 10$ N, Eqs. (3) and (4) yield $m_2 = 0.14$ for a smooth top plate and $m_1 = 0.4$ for a rough top plate. Since the friction coefficients should be independent of the applied force, the result of the analysis for the two normal forces that considers Herschel–Bulkley constitutive equation demonstrates discrepancy. A plausible explanation for observation of a much smaller value of the limiting gap and hence smaller friction coefficients could be the inherent thixotropic character of aqueous suspension of Laponite, which leads to partial shear melting (rejuvenation) at stronger deformation fields (larger forces) reducing viscosity, elastic modulus and yield stress. This time dependent behavior is beyond the scope of Herschel–Bulkley constitutive equation, and therefore it fails to capture the complete behavior for a Laponite suspension which is greatly affected by the strength of deformation field. In addition it is possible that partial shear melting is also playing a role for $F = 2.5$ N experiment. It should be noted that a squeeze flow under no-slip boundary condition involves primarily shear flow in the limit of $d \ll R$ (lubrication approximation) [36,64]. On the other hand, slip on the surface of the plates introduces an elongational flow in addition to the shear flow [29]. As the elongational flow involves a much stronger deformation field than a shear flow, it has been shown to cause a greater extent of deformation induced melting in the sample [65] demonstrating more pronounced thixotropic effect.

For all the subsequent constant force experiments, we have employed a rough top plate to reduce the wall slip. However, bottom plate remains smooth in all our experiments. We first investigate variation of gap between the plates as a function of time under a constant normal force $F = 2.5$ N for different initial gaps between the plates. As shown in an inset of Fig. 4, we observe that even though the constant value of normal force was set at 2.5 N, F fluctuates between 2 and 3 N with mean around 2.5 N. This is because the rheometer maintains the force at an assigned value via a feedback mechanism by controlling the velocity which causes deviations from the set value. Fig. 4 shows that, although the rate of decrease of gap for each initial gap is different, the final value of limiting gap d_L is the same irrespective of the initial gap. The difference in approach of the gap to the limiting value may be due to the fluctuations in the applied force. Interestingly, this observation is in agreement with the prediction of Herschel–Bulkey model represented by Eq. (4), which does not show any dependence of the limiting gap on the initial gap between the plates for constant sample area experiments.

Next we determine the limiting gap d_L at various aging times as shown in Fig. 5. We have employed normal force of $F = 2.5$ N and initial gap of 1000 μm for each aging time dependent experiment. It can be seen that the limiting gap increases with an increase in the sample age. This behavior can be expected to originate from increased yield stress of the sample as a function of aging time shown in Fig. 1. In an inset of Fig. 5, we plot d_L vs. t_w and find that d_L varies as $d_L \sim t_w^{0.42}$. Interestingly, this dependence is again very close to the prediction by Eq. (4), which suggests $d_L \sim \tau_y$, since τ_y is observed to vary according to: $\tau_y \sim t_w^{0.4}$ as shown in Fig. 1. Therefore, at a relatively smaller force of $F = 2.5$ N, both the initial gap variation experiments as well as the aging time dependent experiments may not be causing pronounced deformation induced liquefaction (or significant decrease in viscosity as a function of time over duration of experiment), which leads to reasonable agreement with the Herschel–Bulkley constitutive equation.

We further study effect of magnitude of normal force on the variation of gap as a function of time. Fig. 6 shows that limiting gap follows a power law dependence on force given by $d_L \sim F^{-1.5}$ as shown in the inset. This dependence is stronger than given by Eq. (4), according to which d_L should vary inversely with F. A plausible reason for d_L to be smaller than that predicted by the Herschel–Bulkley model at higher normal forces is pronounced thixotropic effect, which causes an increase in extent of shear melting with an increase in the strength of the deformation field.

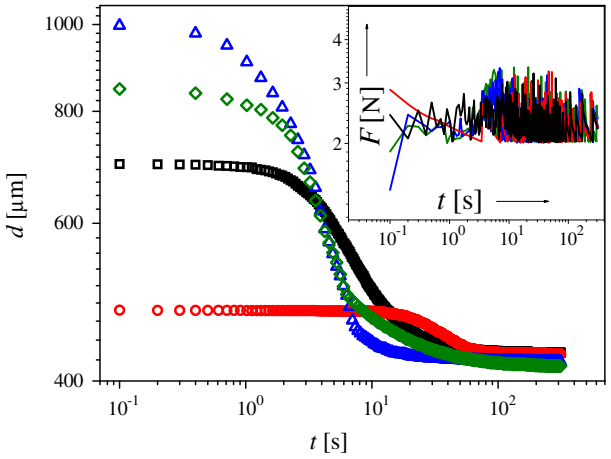

Fig. 4. Gap between the plates (d) as a function of time (t) for different initial gaps [circle, red: 500 μm; square, black: 700 μm; diamond, green: 850 μm; triangle, blue: 1000 μm] between the rough top and smooth bottom plates under the application of a constant force $F = 2.5$ N. The aging time for the each case is $t_w = 15$ min. The limiting gap d_L reached is the same for all the initial gaps. The inset shows F fluctuates around the set value of 2.5 N as a function of time. The colors have the same meaning in both the inset and the main figure. (For interpretation of the references to color in this figure legend, the reader is referred to the web version of this article.)

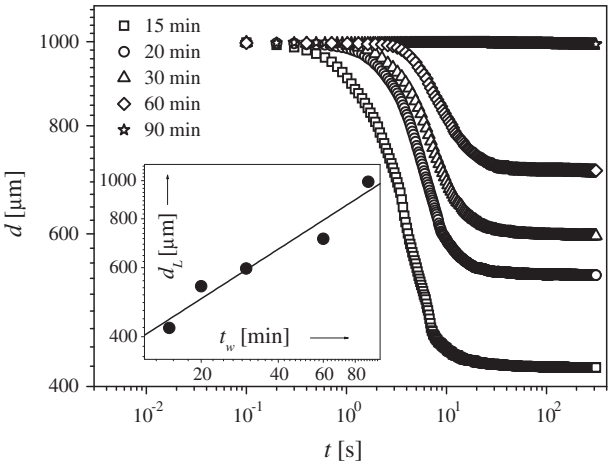

Fig. 5. Gap between the plates (d) as a function of time (t) for different aging times (t_w) under the application of a constant force $F = 2.5$ N. The top and bottom plates are rough and smooth respectively with an initial gap = 1000 μm for all the cases. The inset shows the dependence of limiting gap on aging time ($d_L \sim t_w^{0.42}$) as determined from d vs. t plots shown in the main figure.

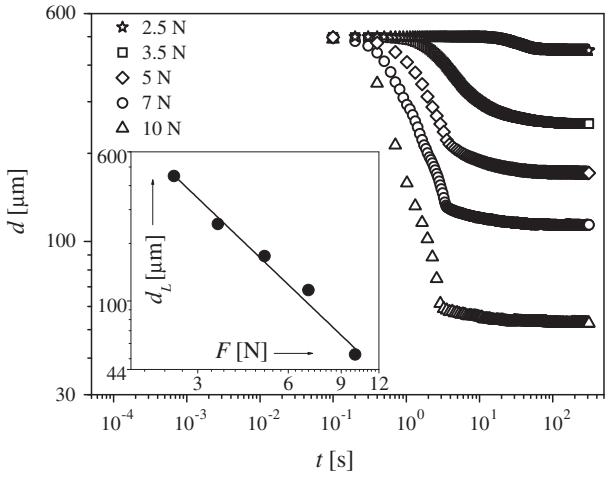

Fig. 6. Variation of gap (d) as a function of time (t) for different values of compressive force (F). The aging time t_w = 15 min, the initial gap is 500 μm. The top plate is rough while the bottom plate is smooth for each force. An inset shows the dependence of limiting gap determined from d vs. t plots shown in the main figure, and is given by $d_L \sim F^{-1.5}$.

Such enhanced fluidity at stronger deformation field reduces yield stress and therefore leads to smaller value of d_L.

In the second part of this work, we discuss the results of velocity (of the top plate) controlled experiments. In this set of experiments we move the top plate with a constant velocity V towards the bottom plate and record the variation of normal force as a function of the gap between the plates. We first study the effect of the nature of the top plate surface by comparing the normal force–gap dependence for rough top plate and smooth top plate as shown in Fig. 7 for V = 10 μm/s and t_w = 15 min. For both the type of plates the normal force increases with a decrease in gap; however, the force is significantly larger at all gaps for a rough plate. In addition, Fig. 7 shows that the slope of the F–d curve is smaller for a smooth plate than for a rough plate. We believe that this behavior is caused by thixotropic effect leading to enhanced deformation induced melting of the sample when a smooth top plate is employed. As discussed earlier, a slip on the surface of the plates introduces an elongational flow in addition to the shear flow which leads to a greater extent of melting or (rejuvenation) in the sample. Consequently, a weaker dependence of the force on gap is observed for smooth plates due to slip.

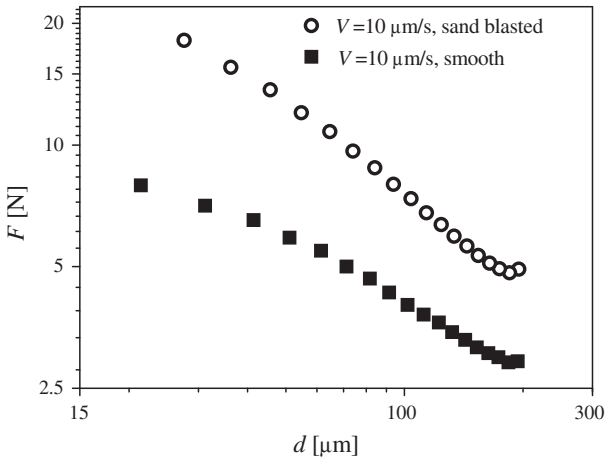

Fig. 7. Variation of the normal force (F) with gap (d) between the plates for rough and smooth top plate for an initial gap of 200 μm. The squeeze velocity (V) is 10 μm/s and the aging time t_w = 15 min. The slope of the curve for smooth top plate is smaller in comparison with rough top plate.

Fig. 8 shows normal force (F) as a function of distance between the plates (d), when the top plate is moved with a constant velocity of 10 μm/s, for various initial gaps between the plates. The age of the sample is 15 min for all the initial gap dependent experiments. It can be seen that over the range of initial gaps explored here (50–700 μm), except for a few initial data points, the variation in normal force as a function of gap between the plates shows identical dependence. Such unique dependence of normal force on plate separation implies that the state of the system is identical for a given inter-plate separation irrespective of the initial gap, given that other parameters like velocity and age remain the same. For Herschel–Bulkley model, normal force is independent of the initial gap (Eq. (A.32)) for a constant sample area experiment. Further, it can be seen that the normal force demonstrates $F \sim d^{-1}$ dependence in the limit of small normal forces (or greater gaps). However, the dependence progressively weakens with a decrease in d as the normal stresses increase. In the limit of low plasticity number, the major resistance to the flow results from yield stress rather than the viscous effects. Therefore, a weak dependence of normal force on gap in the limit of greater normal force appears to be due to partial yielding of a greater portion of the sample that causes decrease in yield stress of the suspension [26]. In an earlier study on filled polydimethylsiloxane, a smaller normal force than that predicted theoretically was also observed by Chan and Baird [20] at smaller gaps for constant velocity experiments. They attributed this discrepancy to a change into a behavior defined by a different set of model parameters at very high shear rates consistent with very small gaps. It was thus concluded that no single set of model parameters could fit the whole range of normal force–gap data. However, we suggest that the present behavior arises from deformation induced melting of the material at smaller gaps when greater extent of normal force acts on the same. This observation also substantiates the behavior reported earlier that aqueous Laponite suspension closely follows Herschel–Bulkley model for small normal forces, however deviates from the same due to thixotropic effects under stronger deformation fields.

In Fig. 9, we plot the normal force as a function of d for experiments carried out at different aging times (t_w). It can be seen that for samples aged for a greater aging time, the normal force is higher at all plate separations. This behavior is expected as increase in age causes enhancement in the yield stress of the material, which offers greater resistance to the deformation. In addition, as observed in Figs. 8 and 9 also shows that the dependence of normal force on d gets weaker with decrease in d.

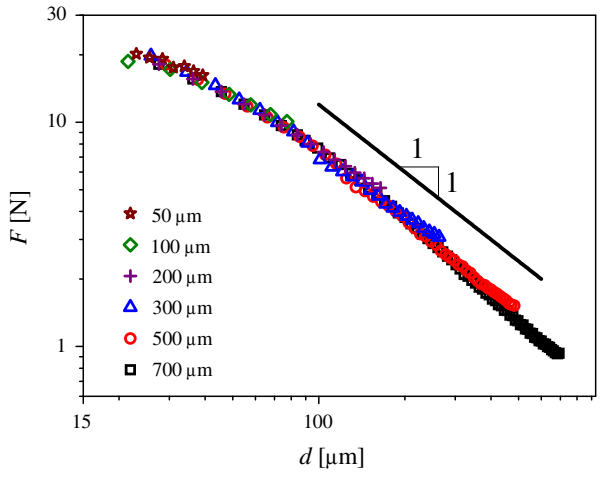

Fig. 8. Normal force (F) as a function of distance between the plates (d) for different initial gaps for the squeeze velocity of 10 μm/s and waiting time of 15 min. The top and bottom plates are rough and smooth respectively.

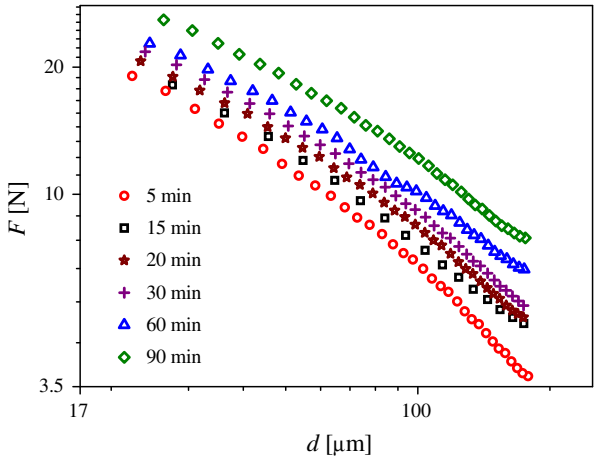

Fig. 9. Normal force (F) plotted as a function of distance between the plates (d) for different aging times (t_w) decreasing from top to bottom. The squeeze velocity is 10 μm/s, initial gap is about 200 μm and the top plate is rough while the bottom plate is smooth for all the tests shown in the figure.

Interestingly, the slope of F–d curve decreases with increased age (t_w) of the sample. The weaker dependence of normal force on d at smaller gaps can be attributed to greater extent of deformation induced melting (decrease in yield stress), as discussed before. On the other hand, the smaller slope of F–d curve at higher age may originate from greater potential of an aged system to demonstrate thixotropic behavior, which is expected to impart greater extent of deformation induced melting in aged samples. Consequently, the nature of the dependence of the data at small age and low gap between the plates closely matches with the same at larger gap and greater age. Such a scenario suggests the possibility of a superposition of the age dependent squeeze flow data by carrying out horizontal shifting of the data as shown in Fig. 10. Inset of the same figure shows that the shift factor a decreases with aging time according to: $a \sim t_w^{-0.26}$. The decrease in horizontal shift factor with aging time suggests equivalence of the dependence of younger sample at small d and older sample at greater d.

Overall, by the virtue of weaker dependence of the normal force on the plate separation at higher age and lower plate separations, self-similarity is observed in the squeeze flow behavior of aqueous suspension of Laponite. Observation of initial gap independent normal force shown in Fig. 8 and superposition of age dependent data shown in Fig. 10 strongly suggest a comprehensive superposition of data obtained for different initial gaps and ages. It can be seen in Fig. 11 that data shown in Figs. 8 and 10 indeed superpose very well, thus further validating the arguments leading to the analysis of the age dependent data. Recently self-similar force–deformation curves were also reported by Rodts and coworkers [66] for a bentonite suspension – also an aging thixotropic soft glassy material – when squeezed at a constant velocity at different aging times. However, contrary to the behavior observed in the present study, their force–deformation curves need shifting on the force axis in order to get the superposition. They attributed this self-similarity to a similar path of changes in the structure followed under deformation irrespective of the aging time. On the other hand, for an aqueous Laponite suspension, we clearly observe different extent of rejuvenation for samples having different ages.

We next examine the results obtained by varying the intensity of the deformation field by varying the velocity of the top plate over two orders of magnitude as shown in Fig. 12. The initial gap and the aging time were kept the same in each experiment at 200 μm and 15 min, respectively. We observe that an increase in

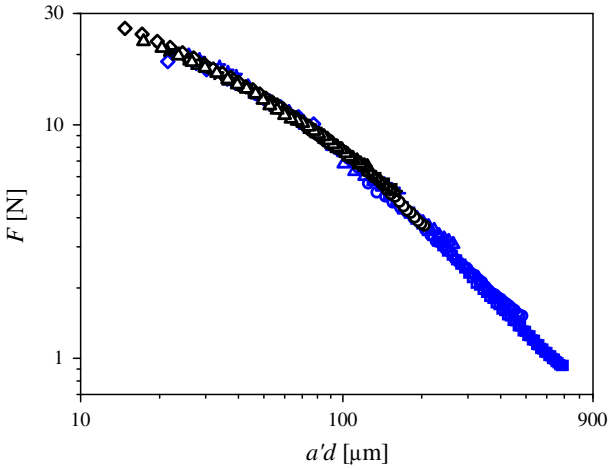

Fig. 11. A comprehensive superposition of initial gap dependent data shown in Fig. 8 (blue symbols) and age dependent data shown in Fig. 10 (black symbols). All the age dependent data curves are shifted onto 15 min data curve. (For interpretation of the references to color in this figure legend, the reader is referred to the web version of this article.)

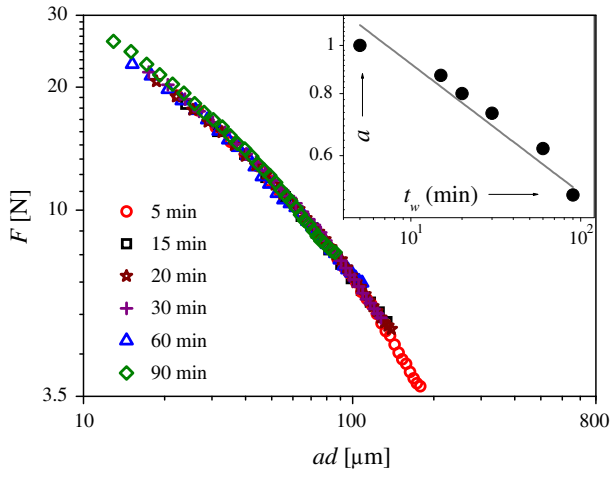

Fig. 10. Superposition of the age dependent data shown in Fig. 9 by carrying out horizontal shifting onto 5 min data curve. Inset shows variation of horizontal shift factor a plotted as a function of aging time ($a \sim t_w^{-0.26}$).

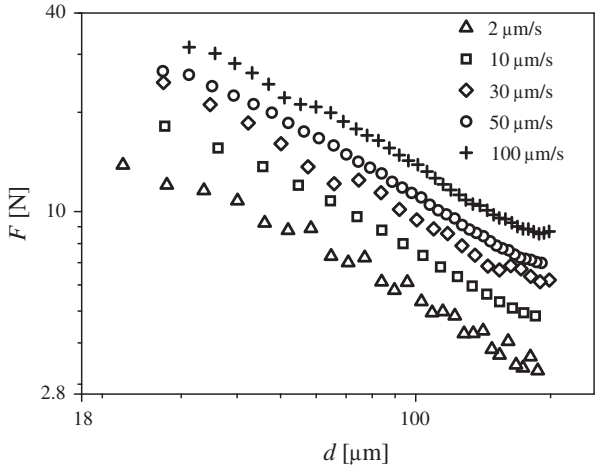

Fig. 12. Normal force (F) as a function of gap (d) obtained for different squeeze velocities for initial gap of 200 μm and waiting time t_w = 15 min. The top plate is rough while the bottom plate is smooth in all the experiments shown here. The magnitude of F is consistently greater at all gaps for larger velocities.

velocity leads to a higher value of normal force at all the values of plate separation. From a Herschel–Bulkley point of view, the yield stress term in Eq. (A.32) does not have any dependence on velocity. However, the second term does have a velocity dependence which can take into account the observed increase in force with velocity. Further, enhanced deformation induced melting at greater velocities, due to decrease in yield stress, might reduce dominance of the first term thereby enhancing viscous contribution.

Overall squeeze flow behavior of a soft glassy material with yield stress that also includes slip on the plate surface is a complex problem due to presence of shear as well as elongational flow on one hand and strong thixotropic behavior (aging and rejuvenation) demonstrated by the material on the other hand. Although, in the limit of weak deformation fields, Herschel–Bulkley fluid appears to explain the rheological behavior, it fails in the limit of strong deformation fields due to thixotropy. Therefore, acknowledging commercial importance of the squeeze flow field and also the soft glassy materials, more theoretical and experimental studies on this system are required.

4. Conclusions

An aqueous suspension of Laponite, which is an important and typical thixotropic soft glassy material with a yield stress, is studied under application of squeeze flow field confined between a rough top plate and a smooth bottom plate. We also extend Sherwood and Durban's [62,63] squeeze flow analysis of Herschel–Bulkley model for two plates having different friction coefficients. In a force controlled mode, gap between the plates decreases as a function of time and eventually attains a plateau value. However, this limiting gap is observed to be smaller when rough top plate is replaced by a smooth top plate. This suggests presence of slip at the plate–sample interface which is more pronounced for a smoother plate. A comparison of the experimental data with the Herschel–Bulkley model enables determination of the friction coefficients at the top and the bottom plates. However, for different normal forces, the model predicts a different set of values of the friction coefficients. We argue that this behavior arises due to thixotropic character of the material wherein a deformation field induces melting (partial yielding or rejuvenation) of Laponite suspension when subjected to strong deformation fields. Since Herschel–Bulkley model does not account for thixotropy, it is inadequate to explain the squeeze flow behavior of soft glassy materials. Nevertheless, for experiments carried out at a relatively smaller force to minimize the effect of rejuvenation, the behavior was found to be independent of the initial gap between the plates while the limiting gap was found to have the same dependence on aging time as that of the yield stress. Both of these observations are in close agreement with the predictions of the Herschel–Bulkley model.

The normal force in the velocity controlled experiments varies inversely with the plate separation as is predicted by a Herschel–Bulkley model. However, at small gaps, the dependence of normal force is observed to deviate from the prediction, which can be attributed to thixotropy causing greater melting of the material with increase in the normal force. Interestingly, thixotropic effects are observed to be pronounced when samples are aged longer and when the gap distances are smaller (or normal force is greater). Similarity of the nature of curves at small ages and at low gaps (and at larger gaps and greater ages) leads to superposition of the aging time dependent normal force vs. plate separation data. An excellent collapse of data on a single master curve clearly demonstrates the self-similarity of the squeeze flow of Laponite suspensions of different ages at different gaps. Furthermore, we observe a higher normal force at all the gaps for larger velocities due to an increased contribution to the normal force from viscous effects. Overall the present work points out the major complexities and their analyses when a thixotropic material with a yield stress is subjected to squeeze flow field. The Herschel–Bulkley model is found to be satisfactory in explaining the squeeze flow behavior for weak deformation fields. On the other hand, for strong deformation fields (high normal stresses, small gaps, and when elongational flow is induced because of partial slip), thixotropic effects play dominating role. In this limit the behavior can be qualitatively explained by accounting for the evolution of the structure with time amidst a competition between the constructive aging and a destructive rejuvenation. We hope that this study of aqueous Laponite suspension under squeeze flow will also lead to new insights into understanding of flow, deformation, and aging and rejuvenation behavior of soft glassy materials in general.

Acknowledgment

Financial support from Department of Science and Technology through an IRHPA Grant is greatly acknowledged.

Appendix A

Sherwood and Durban [62,63] derived an approximate expression for normal force required to bring the two plates together sandwiching a Herschel–Bulkley fluid. They assumed that the shear stress at the sample-plate interface is a fraction m of an effective Mises stress given by

$$\sigma_e^2 = (\sigma_{zz} - \sigma_{rr})^2 + 3\sigma_{rz}^2, \tag{A.1}$$

for the case of $\sigma_{rr} = \sigma_{\theta\theta} \neq \sigma_{zz}$ (for $d \ll R$), where σ_{ij} is a component of stress tensor and r, θ and z are radial, angular and vertical coordinates respectively. They developed the expression for the normal force for the case of the same friction coefficient at both the plates. In this section we extend their analysis in order to derive an expression for the normal force for a different friction coefficient at the top and the bottom plate.

We assume that the two plates are at $z = \pm d/2$ and the top plate approaches the bottom plate with a velocity V while the bottom plate remains fixed. The equations of motion are given by:

$$\frac{\partial \sigma_{rr}}{\partial r} + \frac{\partial \sigma_{rz}}{\partial z} + \frac{\sigma_{rr} - \sigma_{\theta\theta}}{r} = 0, \tag{A.2}$$

$$\frac{\partial \sigma_{rz}}{\partial r} + \frac{\partial \sigma_{zz}}{\partial z} + \frac{\sigma_{rz}}{r} = 0. \tag{A.3}$$

Sherwood and Durban introduced a parameter ψ such that Eq. (A.1) is identically satisfied:

$$\sigma_{rz} = -\frac{\sigma_e \sin\psi}{3^{1/2}}, \tag{A.4}$$

$$\sigma_{rr} - \sigma_{zz} = \sigma_e \cos\psi. \tag{A.5}$$

Substituting $\sigma_{rr} = \sigma_{\theta\theta}$ and integrating Eq. (A.2), they obtained

$$\sigma_{rr} = -\frac{r(\sigma_e \sin\psi)'}{3^{1/2}} + s(z), \tag{A.6}$$

$$\sigma_{zz} = -\frac{r(\sigma_e \sin\psi)'}{3^{1/2}} + s(z) - \sigma_e \cos\psi, \tag{A.7}$$

where prime represents a derivative with respect to z and $s(z)$ is an unknown function of integration. From Eq. (A.3):

$$\frac{r(\sigma_e \sin\psi)''}{3^{1/2}} + s'(z) - (\sigma_e \cos\psi)' - \frac{\sigma_e \sin\psi}{3^{1/2} r} = 0. \tag{A.8}$$

Considering the terms $O(d/r)$ and $O(d/r)^0$ separately and omitting the last term for large r, they obtained:

$$(\sigma_e \sin\psi)'' = 0, \tag{A.9}$$

$$s'(z) - (\sigma_e \cos\psi)' = 0. \tag{A.10}$$

Integration of Eq. (A.9) gives

$$(\sigma_e \sin\psi)' = A, \tag{A.11}$$

$$\sigma_e \sin\psi = Az + B. \tag{A.12}$$

They further derived an expression for σ_e in terms of ψ given by:

$$\sigma_e = \sigma_c \left(\frac{V}{d}\right)^n \frac{1}{(\cos\psi)^n} + 3^{1/2}\tau_y \quad \text{where } \sigma_c = 3^{(1+n)/2}k. \tag{A.13}$$

Using Eq. (A.13), (A.12) can be rewritten as

$$\sigma_c \left(\frac{V}{d}\right)^n \frac{\sin\psi}{(\cos\psi)^n} + 3^{1/2}\tau_y \sin\psi = Az + B, \tag{A.14}$$

where A and B are constants of integration. Let the friction coefficient at the top plate be m_1 and the bottom plate be m_2. Then the boundary conditions are given by:

$$\sigma_{rz} = -\frac{\sigma_e m_1}{3^{1/2}} \text{ at } z = \frac{d}{2} \text{ which gives } \sin\psi = m_1 \text{ at } z = \frac{d}{2} \quad \text{and} \tag{A.15}$$

$$\sigma_{rz} = +\frac{\sigma_e m_2}{3^{1/2}} \text{ at } z = -\frac{d}{2} \text{ which gives } \sin\psi = -m_2 \text{ at } z = -\frac{d}{2}. \tag{A.16}$$

Substituting the above boundary conditions in Eq. (A.14), we obtain the following two equations:

$$\sigma_c \left(\frac{V}{d}\right)^n \frac{m_1}{(1-m_1^2)^{n/2}} + 3^{1/2}\tau_y m_1 = A\frac{d}{2} + B, \tag{A.17}$$

$$-\sigma_c \left(\frac{V}{d}\right)^n \frac{m_2}{(1-m_2^2)^{n/2}} - 3^{1/2}\tau_y m_2 = -A\frac{d}{2} + B, \tag{A.18}$$

which upon solving give,

$$A = \frac{1}{d}\sigma_c \left(\frac{V}{d}\right)^n \left[\frac{m_1}{(1-m_1^2)^{n/2}} + \frac{m_2}{(1-m_2^2)^{n/2}}\right] + \frac{3^{1/2}\tau_y}{d}[m_1 + m_1], \tag{A.19}$$

$$B = \frac{1}{2}\sigma_c \left(\frac{V}{d}\right)^n \left[\frac{m_1}{(1-m_1^2)^{n/2}} - \frac{m_2}{(1-m_2^2)^{n/2}}\right] + \frac{3^{1/2}\tau_y}{2}[m_1 - m_2]. \tag{A.20}$$

Substituting A and B in Eq. (A.14), we obtain the following relation between ψ and z:

$$\frac{\sin\psi}{(\cos\psi)^n} + M\sin\psi = \frac{z}{d}\left[\frac{m_1}{(1-m_1^2)^{n/2}} + \frac{m_2}{(1-m_2^2)^{n/2}} + M(m_1+m_2)\right] + \frac{1}{2}\left[\frac{m_1}{(1-m_1^2)^{n/2}} - \frac{m_2}{(1-m_2^2)^{n/2}} + M(m_1-m_2)\right], \tag{A.21}$$

where $M = \frac{3^{1/2}\tau_y}{\sigma_c}\left(\frac{d}{V}\right)^n$ is a generalized Bingham number.

Integration of Eq. (A.10) gives:

$$s(z) = \sigma_e \cos\psi + C,$$

$$s(z) = \sigma_c \left(\frac{V}{d}\right)^n (\cos\psi)^{1-n} + 3^{1/2}\tau_y \cos\psi + C, \tag{A.22}$$

where C is a constant of integration. Considering outer boundary to be stress free for $m_1, m_2 > 0$,

$0 = \int_{-d/2}^{d/2} \sigma_{rr}\, dz$ at $r = R$, which on substitution of Eq. (A.6) becomes

$$0 = \int_{-d/2}^{d/2} \left[\frac{R(\sigma_e \sin\psi)'}{3^{1/2}} + \sigma_e \cos\psi + C\right] dz. \tag{A.23}$$

Substituting the expression for σ_e (Eq. (A.13)) and from Eq. (A.11), we rewrite Eq. (A.23) as:

$$0 = \frac{RAd}{3^{1/2}} + \sigma_c \left(\frac{V}{d}\right)^n \int_{-d/2}^{d/2} (\cos\psi)^{1-n} dz + 3^{1/2}\tau_y \int_{-d/2}^{d/2} \cos\psi\, dz + Cd. \tag{A.24}$$

Substituting A in the above expression, we get

$$0 = \frac{R}{3^{1/2}}\sigma_c \left(\frac{V}{d}\right)^n \left[\frac{m_1}{(1-m_1^2)^{n/2}} + \frac{m_2}{(1-m_2^2)^{n/2}} + M(m_1+m_2)\right] + Cd + I_{(1-n)}\sigma_c \left(\frac{V}{d}\right)^n d + 3^{1/2}\tau_y I_1 d, \tag{A.25}$$

where $I_\alpha = \frac{1}{d}\int_{-d/2}^{d/2} (\cos\psi)^\alpha dz$ which on simplification gives

$$I_\alpha = \left[\frac{m_1}{(1-m_1^2)} + \frac{m_2}{(1-m_2^2)} + M(m_1+m_2)\right]^{-1} \times \int_{(1-m_2^2)^{1/2}}^{(1-m_1^2)^{1/2}} \frac{Mc^{2+n} + (1-n)c^2 + n}{c^{1+n-\alpha}(1-c^2)^{1/2}} dc. \tag{A.26}$$

From Eq. (A.25):

$$C = -\sigma_c \left(\frac{V}{d}\right)^n \left[\frac{R}{3^{1/2}d}\left(\frac{m_1}{(1-m_1^2)^{n/2}} + \frac{m_2}{(1-m_2^2)^{n/2}} + M(m_1+m_2)\right) + I_{(1-n)} + MI_1\right]. \tag{A.27}$$

The normal stress at $z = d/2$ from Eqs. (A.7) and (A.22):

$$\sigma_{zz} = \frac{rA}{3^{1/2}} + C,$$

$$\sigma_{zz} = \frac{\sigma_c(r-R)}{3^{1/2}d}\left(\frac{V}{d}\right)^n \left[\frac{m_1}{(1-m_1^2)^{n/2}} + \frac{m_2}{(1-m_2^2)^{n/2}} + M(m_1+m_2)\right] - \sigma_c \left(\frac{V}{d}\right)^n [I_{1-n} + MI_1]. \tag{A.28}$$

The force required to push the plates together,

$$F = -2\pi \int_0^R \sigma_{zz} r\, dr$$

$$= -2\pi\left\{\frac{\sigma_c}{3^{1/2}d}\left(\frac{V}{d}\right)^n \left[\frac{m_1}{(1-m_1^2)^{n/2}} + \frac{m_2}{(1-m_2^2)^{n/2}} + M(m_1+m_2)\right]\right\} \times \int_0^R (r^2 - rR)dr - \sigma_c \left(\frac{V}{d}\right)^n [I_{1-n} + MI_1] \int_0^R r\, dr, \tag{A.29}$$

which upon integration gives,

$$F = \frac{\pi R^3 \sigma_c}{d}\left(\frac{V}{d}\right)^n \left[\frac{1}{3^{3/2}}\left\{\frac{m_1}{(1-m_1^2)^{n/2}} + \frac{m_2}{(1-m_2^2)^{n/2}} + M(m_1+m_2)\right\} + \frac{I_{1-n}d}{R} + \frac{MI_1 d}{R}\right]. \tag{A.30}$$

For $m_1^2, m_2^2 \ll 1$, $I_{(1-n)}, I_1 \to 1$, therefore,

$$F = \frac{\pi R^3 \sigma_c}{d}\left(\frac{V}{d}\right)^n \left[\frac{1}{3^{3/2}}\left\{\frac{m_1}{(1-m_1^2)^{n/2}} + \frac{m_2}{(1-m_2^2)^{n/2}} + M(m_1+m_2)\right\} + \frac{d}{R} + \frac{Md}{R}\right]. \tag{A.31}$$

Further for $m_1, m_2 \gg d/R$ (as shown for $m \gg d/R$ by Meeten [18]), the above expression can be written in the following simplified form:

$$F = \frac{\pi\tau_y(m_1+m_2)R^3}{3d} + \frac{\pi k R^3}{3^{1-n/2}d}\left(\frac{V}{d}\right)^n \left[\frac{m_1}{(1-m_1^2)^{n/2}} + \frac{m_2}{(1-m_2^2)^{n/2}}\right]. \tag{A.32}$$

References

[1] M.E. Cates, M.R. Evans, Soft and Fragile Matter, The Institute of Physics Publishing, London, 2000.
[2] D.J. Wales, Energy Landscapes, Cambridge University Press, Cambridge, 2003.
[3] S.A. Rogers, P.T. Callaghan, G. Petekidis, D. Vlassopoulos, Time-dependent rheology of colloidal star glasses, J. Rheol. 54 (2010) 133–158.
[4] D. Bonn, S. Tanasc, B. Abou, H. Tanaka, J. Meunier, Laponite: aging and shear rejuvenation of a colloidal glass, Phys. Rev. Lett. 89 (2002) 157011–157014.
[5] M. Cloitre, R. Borrega, L. Leibler, Rheological aging and rejuvenation in microgel pastes, Phys. Rev. Lett. 85 (2000) 4819–4822.
[6] Y.M. Joshi, G.R.K. Reddy, Aging in a colloidal glass in creep flow: time-stress superposition, Phys. Rev. E 77 (2008) 021501–021504.
[7] Y.M. Joshi, G.R.K. Reddy, A.L. Kulkarni, N. Kumar, R.P. Chhabra, Rheological behavior of aqueous suspensions of Laponite: new insights into the ageing phenomena, Proc. Roy. Soc. A 464 (2008) 469–489.
[8] H.A. Barnes, Thixotropy – a review, J. Non-Newton. Fluid Mech. 70 (1997) 1–33.
[9] P.C.F. Moller, J. Mewis, D. Bonn, Yield stress and thixotropy: on the difficulty of measuring yield stresses in practice, Soft Matter (2006) 274–283.
[10] I.M. Hodge, Physical aging in polymer glasses, Science 267 (1995) 1945–1947.
[11] L.C.E. Struik, Physical Aging in Amorphous Polymers and Other Materials, Elsevier, Houston, 1978.
[12] P. Coussot, H. Tabuteau, X. Chateau, L. Tocquer, G. Ovarlez, Aging and solid or liquid behavior in pastes, J. Rheol. 50 (2006) 975–994.
[13] G. Ovarlez, P. Coussot, Physical age of soft-jammed systems, Phys. Rev. E 76 (2007) 011406.
[14] H.A. Baghdadi, J. Parrella, S.R. Bhatia, Long-term aging effects on the rheology of neat laponite and laponite – PEO dispersions, Rheol. Acta 47 (2008) 349–357.
[15] S.M. Fielding, P. Sollich, M.E. Cates, Aging and rheology in soft materials, J. Rheol. 44 (2000) 323–369.
[16] J. Engmann, C. Servais, A.S. Burbidge, Squeeze flow theory and applications to rheometry: a review, J. Non-Newton. Fluid Mech. 132 (2005) 1–27.
[17] S.L. Kieweg, D.F. Katz, Squeezing flows of vaginal gel formulations relevant to microbicide drug delivery, J. Biomech. Eng. 128 (2006) 540–553.
[18] G.H. Meeten, Constant-force squeeze flow of soft solids, Rheol. Acta 41 (2002) 557–566.
[19] G. Karapetsas, J. Tsamopoulos, Transient squeeze flow of viscoplastic materials, J. Non-Newton. Fluid Mech. 133 (2006) 35–56.
[20] T.W. Chan, D.G. Baird, An evaluation of a squeeze flow rheometer for the rheological characterization of a filled polymer with a yield stress, Rheol. Acta 41 (2002) 245–256.
[21] H.M. Laun, M. Rady, O. Hassager, Analytical solutions for squeeze flow with partial wall slip, J. Non-Newton. Fluid Mech. 81 (1999) 1–15.
[22] A. Lawal, D.M. Kalyon, Squeezing flow of viscoplastic fluids subject to wall slip, Polym. Eng. Sci. 38 (1998) 1793–1804.
[23] P. Shirodkar, A. Bravo, S. Middleman, Lubrication flows in viscoelastic liquids – 2. Effect of slip on squeezing flow between approaching parallel rigid planes, Chem. Eng. Commun. 14 (1982) 151–175.
[24] G.G. Lipscomb, M.M. Denn, Flow of Bingham fluids in complex geometries, J. Non-Newton. Fluid Mech. 14 (1984) 337–346.
[25] C.J. Lawrence, G.M. Corfield, Non-viscometric flow of viscoplastic materials: squeeze flow, Dynam. Complex Fluids (1998) 379–393.
[26] M.M. Denn, Are plug-flow regions possible in fluids exhibiting a yield stress?, in: M.J. Adams, R.A. Mashelkar, J.R.A. Pearson, A.R. Rennie (Eds.), Dynamics of Complex Fluids, Imperial College Press, London, 1998, pp. 372–378.
[27] G.H. Meeten, Radial filtration during constant-force squeeze flow of soft solids, Rheol. Acta 46 (2007) 803–813.
[28] G.H. Covey, B.R. Stanmore, Use of the parallel-plate plastometer for the characterisation of viscous fluids with a yield stress, J. Non-Newton. Fluid Mech. 8 (1981) 249–260.
[29] G.H. Meeten, Squeeze flow of soft solids between rough surfaces, Rheol. Acta 43 (2004) 6–16.
[30] F. Yang, Exact solution for compressive flow of viscoplastic fluids under perfect slip wall boundary conditions, Rheol. Acta 37 (1998) 68–72.
[31] P. Estellé, C. Lanos, Squeeze flow of Bingham fluids under slip with friction boundary condition, Rheol. Acta 46 (2007) 397–404.
[32] B.D. Rabideau, C. Lanos, P. Coussot, An investigation of squeeze flow as a viable technique for determining the yield stress, Rheol. Acta 48 (2009) 517–526.
[33] G.H. Meeten, Yield stress of structured fluids measured by squeeze flow, Rheol. Acta 39 (2000) 399–408.
[34] G.H. Meeten, Effects of plate roughness in squeeze-flow rheometry, J. Non-Newton. Fluid Mech. 124 (2004) 51–60.
[35] R.B. Bird, R.C. Armstrong, O. Hassager, Dynamics of Polymeric Liquids, Fluid Mechanics, vol. I, Wiley-Interscience, New York, 1987.
[36] P. Coussot, Rheometry of Pastes, Suspensions and Granular Materials – Application in Industry and Environment, Wiley, Hoboken, 2005.
[37] G. Ovarlez, Q. Barral, P. Coussot, Three-dimensional jamming and flows of soft glassy materials, Nat. Mater. 9 (2010) 115–119.
[38] H.A. Barnes, The yield stress—a review or 'panta roi'—everything flows?, J Non-Newton. Fluid Mech. 81 (1999) 133–178.
[39] Q.D. Nguyen, D.V. Boger, Measuring the flow properties of yield stress fluids, Annu. Rev. Fluid. Mech. 24 (1992) 47–88.
[40] A. Mujumdar, A.N. Beris, A.B. Metzner, Transient phenomena in thixotropic systems, J. Non-Newton. Fluid Mech. (2002) 157–178.
[41] D.C.-H. Cheng, Characterisation of thixotropy revisited, Rheol. Acta 42 (2003) 372–382.
[42] P. Coussot, Q.D. Nguyen, H.T. Huynh, D. Bonn, Viscosity bifurcation in thixotropic, yielding fluids, J. Rheol. 46 (2002) 573–589.
[43] J.R. Seth, R.T. Bonnecaze, M. Cloitre, Influence of short-range forces on wall-slip in microgel pastes, J. Rheol. 52 (2008) 1241.
[44] Available from: www.laponite.com.
[45] A.S. Negi, C.O. Osuji, Time-resolved viscoelastic properties during structural arrest and aging of a colloidal glass, Phys. Rev. E 82 (2010) 031404.
[46] V. Awasthi, Y.M. Joshi, Effect of temperature on aging and time–temperature superposition in nonergodic laponite suspensions, Soft Matter 5 (2009) 4991–4996.
[47] R. Bandyopadhyay, H. Mohan, Y.M. Joshi, Stress relaxation in aging soft colloidal glasses, Soft Matter 6 (2010) 1462–1466.
[48] A. Shahin, Y.M. Joshi, Irreversible aging dynamics and generic phase behavior of aqueous suspensions of Laponite, Langmuir 26 (2010) 4219–4225.
[49] H.A. Baghdadi, E.C. Jensen, N. Easwar, S.R. Bhatia, Evidence for re-entrant behavior in Laponite-PEO systems, Rheol. Acta 47 (2008) 121–127.
[50] R. Bandyopadhyay, D. Liang, J.L. Harden, R.L. Leheny, Slow dynamics, aging, and glassy rheology in soft and living matter, Solid State Commun. 139 (2006) 589–598.
[51] D. Bonn, P. Coussot, H.T. Huynh, F. Bertrand, G. Debregeas, Rheology of soft glassy materials, Europhys. Lett. 59 (2002) 786–792.
[52] B. Abou, D. Bonn, J. Meunier, Aging dynamics in a colloidal glass, Phys. Rev. E 64 (2001) 215101–215106.
[53] B. Abou, F. Gallet, Probing a nonequilibrium Einstein relation in an aging colloidal glass, Phys. Rev. Lett. 93 (2004) 160603.
[54] A. Shahin, Y.M. Joshi, Prediction of long and short time rheological behavior in soft glassy materials, Phys. Rev. Lett. 106 (2011).
[55] H.A. Baghdadi, S.R. Bhatia, E.E.C. Jensen, N. Easwar, Evidence of re-entrant behavior in Laponite-PEO systems, in: Materials Research Society Symposium Proceedings, 2005, pp. 188–192.
[56] S. Bhatia, J. Barker, A. Mourchid, Scattering of disklike particle suspensions: evidence for repulsive interactions and large length scale structure from static light scattering and ultra-small-angle neutron scattering, Langmuir 19 (2003) 532–535.
[57] M. Kroon, W.L. Vos, G.H. Wegdam, Structure and formation of a gel of colloidal disks, Phys. Rev. E 57 (1998) 1962–1970.
[58] A. Mourchid, P. Levitz, Long-term gelation of Laponite aqueous dispersions, Phys. Rev. E 57 (1998) R4887–R4890.
[59] Y.M. Joshi, Model for cage formation in colloidal suspension of Laponite, J. Chem. Phys. 127 (2007) 081102.
[60] P. Coussot, Rheophysics of pastes: a review of microscopic modelling approaches, Soft Matter 3 (2007) 528–540.
[61] G.H. Meeten, Comparison of squeeze flow and vane rheometry for yield stress and viscous fluids, Rheol. Acta 49 (2010) 45–52.
[62] J.D. Sherwood, D. Durban, Squeeze-flow of a Herschel–Bulkley fluid, J. Non-Newton. Fluid Mech. 77 (1998) 115–121.
[63] J.D. Sherwood, D. Durban, Squeeze flow of a power-law viscoplastic solid, J. Non-Newton. Fluid Mech. 62 (1996) 35–54.
[64] W.M. Deen, Analysis of Transport Phenomena, Oxford University Press, New York, 1998.
[65] A. Shaukat, A. Sharma, Y.M. Joshi, Time-aging time-stress superposition in soft glass under tensile deformation field, Rheol. Acta 49 (2010) 1093–1101.
[66] S. Rodts, J. Boujlel, B. Rabideau, G. Ovarlez, N. Roussel, P. Moucheront, C. Lanos, F. Bertrand, P. Coussot, Solid–liquid transition and rejuvenation similarities in complex flows of thixotropic materials studied by NMR and MRI, Phys. Rev. E 81 (2010) 021402.